FINAL REPORT

Title: A comparison and development of methods for estimating sagebrush shrub biomass and fuels

JFSP PROJECT ID: 22-1-01-4

09/2024

Eva K. Strand
University of Idaho

Georgia R. Harrison
University of Idaho

FIRESCIENCE.GOV
Research Supporting Sound Decisions

Project ID: **22-1-01-4** Status: **Final**

Title: **A comparison and development of methods for estimating sagebrush shrub biomass and fuels**

Principal Investigator: **Eva K. Strand**

Student Investigator: **Georgia R. Harrison**

Agency/Organization: **University of Idaho, College of Natural Resources**

Reporting Year	**2024**
Final Report Due Date	**8-31-24**
Unspent Funds	**$0**

Project Status

This project is completed, including data collection, analysis, results, and publication.

Deliverables

Deliverable	Description	Status and Completion
Progress report	Annual JFSP progress report	Submitted
Fact sheet	Species-specific shrub allometric biomass equations to be shared with managers via the JFSP Fire Science Exchange Network	We did not end up writing up a fact sheet. Instead, we wrote refereed publication which is currently under revision in REM: Harrison GR, Bourne A, Ellsworth LM, Shaff SE, Hulet A, Strand EK. Allometric relationships to calculate aboveground biomass for eight rangeland shrubs using the SageSTEP network. In Revisions in *Rangeland Ecology & Management*.
Webinar/training session	Webinar delivered via Great Basin Fire Science Exchange (GBFSE), including an explanation of tools (Table 3)	A webinar has not yet been scheduled. Instead, we will be presenting this information as a 15 min conference presentation at the upcoming Society for Range Management meeting (February

		2025, Spokane, WA). Harrison GR, Bourne A, Ellsworth LM, Shaff SE, Hulet A, Strand AK. Allometric relationships to calculate aboveground biomass for eight rangeland shrubs using the SageSTEP network.
Conference presentation	Present results on UAV-based biomass estimates and how these compare to other methods	Harrison GR, Shrestha A, Karl JW. 2023. Seeing shrubs from the sky: an exploration of using drone-based methods to estimate shrub canopy volume. Ecological Society of America annual meeting (Portland, OR, USA).
Dissertation chapter	Will include this project as a chapter in my dissertation	Harrison, Georgia R. 2023. Controlling Annual Grasses in Sagebrush Communities With Higher Resistance and Resilience Is Crucial to Prevent Fire Risk and Invasion Expansion. PhD Dissertation, Department of Plant Science, University of Idaho, Moscow, ID, USA.
Refereed publication	Methods paper published in *Rangelands* or *Fire Ecology*	We created two refereed publications from this project. One is published already, and the second is under review (has already undergone one round of peer review). Harrison, G.R., A. Shrestha, E.K. Strand, J.W. Karl. 2024**.** A comparison and development of methods for estimating shrub volume using drone-imagery-derived point clouds. Ecosphere, 15(5): e4877. https://doi.org/10.1002/ecs2.4877 Harrison GR, Bourne A, Ellsworth LM, Shaff SE, Hulet A, Strand EK. Allometric relationships to calculate aboveground biomass for eight rangeland shrubs using the SageSTEP network. In Revisions in *Rangeland Ecology & Management*.

Metadata

We plan to use the JFSP-recommended repository (Forest Service Research Data Archive). Data has not yet been uploaded. We are working towards meeting these requirements.

Other products

Key findings will be entered into the *Findings tab* as part of the submission of the final report submission.

Photographs

Photographs will be entered into the *Photograph category* as part of the submission of the final report submission.

Project Overview

Estimating canopy volume of shrubs in rangeland ecosystems is important for calculating shrub biomass, fuel loading, wildlife habitat, site productivity, and ecosystem structure. Field techniques for biomass estimation, including destructive sampling, ocular estimates, and allometric techniques, use shrub height and canopy widths to estimate volume and translate it to biomass. These techniques are time-consuming and pose challenges, including removal of plant material and training of observers. In this project we sought to expand techniques and methodologies for estimating canopy volume using two main techniques: drone imagery and additional allometric equations. First, we used drone imagery and structure-from-motion photogrammetry to estimate shrub canopy volume for seven dominant species in southern Idaho, achieving strong correlations with field measurements ($R^2 > 0.9$ for larger shrubs). These drone-based methods were less time-consuming, reduced user variability, and was better suited for large-scale applications compared to traditional techniques, though we did observe slight overestimation of canopy volume for smaller shrubs (canopy diameter <1 m). We also demonstrated a proof of concept for automating canopy volume estimates using point-cloud-based automatic shrub detection algorithms. We suggest that drone-based models provide a suitable alternative to field methods, while having the added benefit of being less time-consuming, with fewer limitations, and more easily scaled to larger study areas than traditional field techniques. Secondly, we sought to expand the availability (species and geographic extent) of field-derived allometric equations. Allometric equations employ a double sampling technique, which correlates destructively sampled biomass measurements with field-measured height and canopy size. We created new allometric equations for eight shrubland species and span a range of site conditions, we sampled 631 shrubs of eight species at 13 sites in the Great Basin within the Sagebrush Steppe Treatment Evaluation Project (SageSTEP) monitoring network. This effort generated both generalized species-specific and site-specific biomass equations through linear regression models. This dual modeling approach offers users the flexibility to apply general species relationships or tailor biomass estimation based on geographical location or species distribution.

Additionally, our research provides biomass estimates within fuel size classes, enhancing the utility of these equations for future research and management applications in the Great Basin (Figure 5). Together, these advancements demonstrate that integrating drone-based methods with enhanced allometric equations offers robust, efficient, and versatile tools for monitoring and managing shrub ecosystems.

Font Matter

Table of contents

List of Tables

List of Figures

Key words: Canopy volume, digital photogrammetry, fuel load, rangeland, sagebrush, Structure-from-motion, unmanned aerial system (UAS), vegetation monitoring, fuel loading, bulk density, sagebrush, shrubland, plant allometry, Artemisia tridentata.

Acknowledgments: Thanks to Caroline Ludwig for helping with early analysis and draft writing and to Lisa Jones, Kayla Johnston, Fisher Reis, Savannah Reed, and Kaemen West for their assistance with field work. Also, thanks to Tim Prather, Lisa Jones, and Lisa Ellsworth for their advice and review of this project.

Abstract

Shrub volume is used to calculate numerous, essential ecological indicators in rangeland ecosystems such as biomass, fuel loading, wildlife habitat, site productivity, and ecosystem structure. Field techniques for biomass estimation, including destructive sampling, ocular estimates, and allometric techniques use shrub height and canopy widths to estimate volume and translate it to biomass with species-specific allometric equations. These techniques are time-consuming, and pose challenges, including removal of plant material and training of observers. In this project we sought to expand techniques and methodologies for estimating canopy volume using two main techniques: drone imagery and additional allometric equations. First, we compared canopy volume estimates from field-based measurements with drone-collected canopy volume estimates for seven dominant shrub species within mountain big sagebrush (*Artemisia tridentata* subsp. *vaseyana*) plant communities in southern ID, USA. Canopy height and two perpendicular width measurements were taken from 103 shrubs of varying sizes, and volume was estimated using a traditional allometric equation. Overlapping aerial images captured with a DJI Mavic 2 Professional drone were used to create a 3D representation of the study area using structure-from-motion photogrammetry. Each shrub was extracted from the point cloud, and volume was estimated using allometric and volumetric methods. The volumetric method, which involved converting point clouds to raster canopy height models with 2.5 and 5 cm grid cells, outperformed the allometric method ($R2 > 0.7$), and was more reproducible and robust to user-related variability. Drone-estimated volume best matched field-estimated volume ($R2 > 0.9$) for three larger species: *A. tridentata* subsp. *tridentata*, *A. tridentata* subsp. *vaseyana*, and *Purshia tridentata*. The volume of smaller shrubs (canopy widths <1 m) was slightly overestimated from drone-based models. Second, we created new allometric equations for eight shrubland species and span a range of site conditions using a sample of 631 shrubs of eight species at 13 sites in the Great Basin within the Sagebrush Steppe Treatment Evaluation Project (SageSTEP) monitoring network. This effort generated both generalized species-specific and site-specific biomass equations through linear regression models. This dual modeling approach offers users the flexibility to apply general species relationships or tailor biomass estimation based on geographical location or species distribution. Additionally, we provide biomass estimates within fuel size classes, enhancing the utility of these equations for future research and management applications in the Great Basin. Our equations are shared as R code and an excel sheet, allowing users to implement these equations. Our findings from these two experiments demonstrate that drone-collected images can be used to assess shrub canopy volume for at least five upland sagebrush steppe shrub species and support the integration of drone data-collection into rangeland vegetation monitoring. Further, by advancing the availability and precision of allometric equations for upland shrub species, our study contributes valuable tools for understanding shrub biomass dynamics in sagebrush shrubland ecosystems.

Objectives

1. Create predictive regression models to determine site- and species-specific shrub biomass using height and crown measurement from existing SageSTEP data
    a. Objective met, results shared during conference presentations and within a refereed publication:
        i. Conference presentation: Harrison GR, Bourne A, Ellsworth LM, Shaff SE, Hulet A, Strand AK. 2025. Allometric relationships to calculate

aboveground biomass for eight rangeland shrubs using the SageSTEP network. Society for Range Management annual meeting, Spokane, WA, USA.

ii. Refereed publication: Harrison GR, Bourne A, Ellsworth LM, Shaff SE, Hulet A, Strand EK. Allometric relationships to calculate aboveground biomass for eight rangeland shrubs using the SageSTEP network. In Revisions in Rangeland Ecology & Management.

2. Independently validate regression models using double sampling technique to assess model fit in alternate sites and species
    a. Objective not explicitly met. We instead relied on existing field datasets (objective 1) and proposed alternative methods for calculating shrub canopy volume using UAVs (objective 2).
3. Assess suitability of surveying shrub volume using an Unmanned Aerial Vehicle (UAV) compared to in situ measurements for future research and monitoring efforts
    a. Objective met, results shared during conference presentations and within a refereed publication:
        i. Conference presentation: Harrison GR, Shrestha A, Karl JW. 2023. Seeing shrubs from the sky: an exploration of using drone-based methods to estimate shrub canopy volume. Ecological Society of America annual meeting (Portland, OR, USA).
        ii. Refereed publication: Harrison, G.R., A. Shrestha, E.K. Strand, J.W. Karl. 2024. A comparison and development of methods for estimating shrub volume using drone-imagery-derived point clouds. Ecosphere, 15(5): e4877. https://doi.org/10.1002/ecs2.4877

Background

There are numerous techniques used to estimate shrub biomass and fuel loading. Broadly, these methods are either destructive or non-destructive and can be implemented individually or through double sampling. Destructive sampling requires shrubs to be cut at the base, dried in a forced-air oven at 60-70 °C for at least 24-48 hours and weighed (Rittenhouse and Sneva 1977). Destructive sampling is the most accurate way to measure biomass and does not require extensive training for observers. However, it is time consuming and laborious, especially if biomass by fuel size class is required, and can be difficult to implement in remote areas and with large shrubs.

Non-destructive sampling includes multiple techniques: relative estimates, percent cover translation, and allometric relationships. Relative estimates involve weighing representative units of a plant (e.g., a branch), and training observers to recognize these “weight units” within the sample area or on an individual shrub. Relative estimates can allow for a larger sample size but extensive training and skill within observers is required. Biomass can also be translated from percent cover values, as implemented by Riccardi et al. (2007) in their guide to characterize wildland fuel beds. The primary technique used to non-destructively sample shrub biomass is through creating allometric relationships between canopy volume or other attributes of shrub size (i.e. height, canopy width) to biomass. Shrub height and two perpendicular longest crown intercepts are measured and converted to canopy volume based on shrub shape (Rittenhouse and Sneva, 1977; Uresk et al., 1997).

Unmanned aerial vehicles (UAVs, i.e., drones) can also be used for non-destructive shrub sampling. Several studies have demonstrated the high value of drone-acquired imagery for sampling vegetation attributes (i.e. Cunliffe et al. 2016; Gillian et al. 2019; Karl et al. 2020; Cunliffe et al. 2021). The availability of low-cost consumer UAVs with high-quality imaging sensors makes it possible to collect very-high-resolution imagery easily and inexpensively. Further, new photogrammetric techniques can create high-quality 3-dimensional models and orthomosaics from drone imagery (Westoby et al. 2012). Altogether, this has up new possibilities for using drones as a supplement or replacement for field measurement methods, as demonstrated by Karl et al. (2020) in their measurements of willow canopy volume using drone-collected images and by Cunliffe et al. (2021) in estimating above-ground biomass of vegetation in arid ecosystems.

Double sampling facilitates the integration of two distinct methods by first requiring the measurement of a specific attribute for all individuals using one quick sampling technique. Non-destructive techniques such as measuring shrub size or recording foliar cover are often implemented at this stage. Then, a selected subset of the individuals is reevaluated using a different, often more time-consuming and labor-intensive method. Destructive sampling techniques are often implemented for this subset sample. Although the sub-sampled technique demands additional resources, it enhances overall accuracy. To establish predictive models, a correlation between the outcomes of the sub-sample and the entire sample is derived. Linear regression analysis is typically employed to elucidate the relationship between the two sampling techniques, and the model's predictive capacity is validated using reserved or new data. This approach offers the advantage of leveraging the precision of more intensive methods while extending applicability to a broader context, thereby enhancing feasibility. Double sampling techniques find frequent application in estimating shrub biomass, exemplified by the work of Uresk et al. (1997) as well as Rittenhouse and Sneva (1977), who employed this method in developing biomass equations for *Artemisia tridentata* Nutt.

Materials and Methods

A comparison and development of methods for estimating shrub volume using drone imagery-derived point clouds

This study was conducted at the University of Idaho's Rinker Rock Creek Ranch in southern Idaho (43.4139 °N, 114.3946 °W). The 9-ha study area was located on the south end of the ranch and was selected due to abundance of multiple shrub species, and accessibility for drone flights and field measurements. Eight species of shrubs from upland sagebrush shrublands were included in this study: low sagebrush (*Artemisia arbuscula*), basin big sagebrush (*Artemisia tridentata* subsp. *tridentata*), mountain big sagebrush (*Artemisia tridentata* subsp. *vaseyana*), Wyoming big sagebrush (*Artemisia tridentata* subsp. *wyomingensis*), yellow rabbitbrush (*Chrysothamnus viscidiflorus*), rubber rabbitbrush (*Ericameria nauseosa*), antelope bitterbrush (*Purshia tridentata*), and spineless horsebrush (*Tetradymia canescens*). 2 - 15 individuals of each shrub species were identified within the study area, for a total of 105 shrubs (Table 1). Individuals were selected to represent the range of sizes for each species observed at the site. Only two individuals of *A. tridentata* subsp. *tridentata* were sampled due to limited abundance at the site.

Two individuals, both *P. tridentata*, were larger than all other samples with field measured volumes of 7.94 and 7.27 m^3. We performed a z-test for outliers and both shrubs were

significant outliers (z-scores = 6.21 and 6.81, respectively). As such, these two individuals were removed from further analysis, and summary statistics are reported with and without these two individuals in Table 1.

Table 1. Descriptive summary (mean and range) of field measurements for shrub sampling.

Species	n	Height (m)	D_1 (m)	D_2 (m)	Volume (m^3)
A. arbuscula	15	0.43 [0.24 – 0.60]	0.81 [0.49 – 1.36]	0.62 [0.21 – 1.52]	0.15 [0.02 – 0.54]
A. tridentata ssp. *tridentata*	2*	1.27 [0.99 – 1.54]	1.63 [1.09 – 2.17]	0.96 [0.70 – 1.22]	1.27 [0.40 – 2.13]
A. tridentata ssp. *vaseyana*	15	0.70 [0.52 – 1.02]	1.03 [0.45 – 1.65]	0.89 [0.43 – 1.59]	0.41 [0.07 – 1.10]
A. tridentata ssp. *wyomingensis*	14	0.54 [0.32 – 0.87]	0.76 [0.43 – 1.56]	0.50 [0.19 – 1.21]	0.157 [0.01 – 0.86]
C. viscidiflorus	14	0.36 [0.19 – 0.49]	0.51 [0.24 – 0.69]	0.36 [0.15 – 0.55]	0.04 [0.004 – 0.07]
E. nauseosa	15	0.50 [0.20 – 0.82]	0.79 [0.23 – 1.73]	0.67 [0.17 – 2.50]	0.20 [0.01 – 0.96]
P. tridentata$_1$	15	1.00 [0.31 – 1.78]	1.57 [0.75 – 3.34]	1.31 [0.54 – 2.55]	1.76 [0.07 – 7.94]
P. tridentata$_2$	13	0.88 [0.31 – 1.53]	1.30 [0.75 – 2.03]	1.12 [0.54 – 2.05]	0.86 [0.07 – 2.63]
T. canescens	15	0.37 [0.28 – 0.46]	0.62 [0.31 – 0.97]	0.48 [0.22 – 0.70]	0.06 [0.01 – 0.16]

* only two individuals of *A. tridentata* subsp. *tridentata* were able to be sampled due to limited abundance at the site; this species was excluded from species-specific examinations.

$_{1, 2}$ with *P. tridentata* denotes inclusion and exclusion of large (field volume >7 m^3) shrubs, respectively

Upon selection, shrubs were marked with plastic flagging tape and assigned a unique identifying number. Tallest height and two perpendicular canopy widths for each shrub were measured to the nearest whole centimeter using a 2-m ruler (Fig. 1).

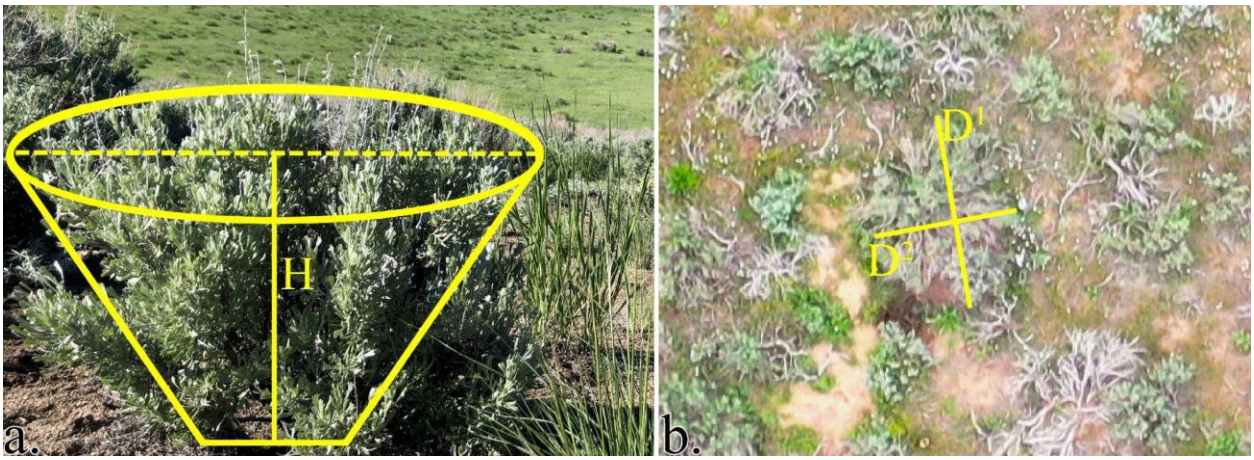

Figure 1. Shrub canopy volume was estimated from field-collected data on shrub maximum height (a) and two measures of canopy width (yellow; b) following Bourne & Bunting (2011). H is shrub height, D_1 is the longest canopy width, and D_2 is the greatest canopy width perpendicular to D_1.

From height and canopy widths, canopy volume was calculated for each individual shrub. First, following Karl et al. (2020), canopy volume was calculated using the equation for an ellipsoid modified by Thorne et al. (2002): $V = \frac{2}{3}\pi * H * \frac{D_1 * D_2}{2}$, where H is shrub height, D_1 is the longest canopy diameter, and D_2 is the longest diameter perpendicular to D_1 (Fig. 2). However, initial data exploration indicated a poor fit between field and drone-based measurements, therefore an alternative shape for volume calculation was considered for this project Canopy volume was then calculated using the equation for volume of an elliptical cone: $V = \frac{\pi}{6} H * D_1 * D_2$.

To prepare for drone flights and improve model accuracy at predicting ground elevation and thus plant height (see Karl et al. 2020), vegetation at the base of each shrub was removed. Point locations surrounding each individual shrub (four corners) were collected using an Emlid Reach RS+ real-time kinematic geographic navigation satellite system (RTK-GNSS) (absolute accuracy < 4cm, Emlid, https://emlid.com), to aid in identification of each shrub in final image products.

Drone flights took place on June 27, 2022. The imaged area was established in the field, and a double-overlap grid pattern consisting of parallel flight lines in north-south and east-west directions was created. We flew a DJI Mavic 2 Pro drone with a 20-megapixel RGB camera 50 meters above ground level. Images collected during drone flights had at least 80% endlap and sidelap. This drone flight resulted in 1,302 images.

Seventeen ground control points (GCPs) were placed throughout the study area to improve model building, point cloud and orthomosaic accuracy and scaling, and identification of shrubs in the point clouds and orthomosaics. Precise location (absolute accuracy < 4cm) of each marker was recorded using the Emlid Reach RS+ RTK-GNSS. All RTK-GNSS points (one for each GCPs and four for each shrub) were post-processed using rover and base tracking within Emlid Studio version 1.3 (https://docs.emlid.com/emlid-studio) for point correction.

The photos collected from the drone were used to produce a point cloud, digital elevation model, and orthomosaic using structure-from-motion (SfM) photogrammetry in Agisoft

Metashape Professional (version 1.8.4 build 14671; herein referred to as 'Metashape'). A SfM-based approach allows for the creation of a stereo model that represents the orientation and location of the drone camera for every collected photo and a 3-dimensional (3D) model of the area photographed (Westoby et al., 2012). The photo processing workflow in Metashape followed methods outlined by James et al. (2017) and implemented by Karl et al. (2020). All 1,302 photos were imported and aligned with Metashape's highest accuracy setting and a maximum of 40,000 key points (unique points detected in an image that potentially appear in other images of the photoset) and 6,000 tie points (points that are common in overlapping images of the photoset) per image.

The post-processed locations of the GCPs were imported into Metashape as markers for geolocation and scaling of the stereo model. Marker locations were identified and manually adjusted for at least 20 photos per marker. Stereo model alignment parameters were re-optimized with adaptive model fitting and tie point covariance estimations based on the manually assigned marker locations. The sparse cloud representing the tie point locations was then optimized using the 'gradual selection' tool in Metashape to select and remove low-quality tie points followed by re-optimization of the photo bundle-block following techniques outlined by James et al. (2017). Marker corrections and sparse point cloud optimization reduced positional errors in X, Y, and Z from 1.03, 1.06, and 2.19 to 0.04, 0.03, and 0.47 m respectively, and reduced the total positional error from 2.64 to 0.48 m.

After model optimization, a dense point cloud was generated in Metashape using the optimized sparse point cloud as the base model with 'high' quality and 'mild' point filtering options. The dense cloud contained over 311 million points (~2,020 points/m^2). A digital elevation model (DEM) was created based on the dense point cloud with a resolution of 2.22 cm/pix, and an orthomosaic was generated based on the DEM product.

The orthomosaic generated from Metashape was displayed in ArcGIS Pro (V 3.0.2, ESRI, Redlands, CA; herein referred to as 'ArcGIS') using NAD83/UTM zone 11N coordinate reference system (EPSG:26911). The post-processed locations representing the four points surrounding each shrub were also imported onto ArcGIS. These points were used as guides to manually digitize areas of interest (AOIs) around each shrub (Fig. 2). Once all the sampled sample shrub boundaries were manually digitized, a polygon feature class containing a total of 105 AOIs (individual polygons) was exported as a shapefile.

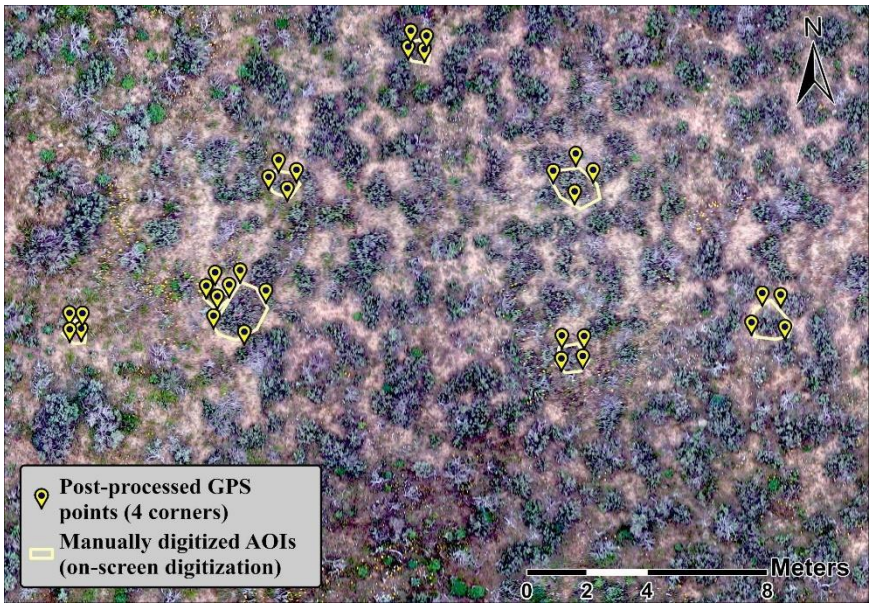

Figure 2. Four corners (yellow points) around each shrub (from post-processed point locations) overlaid on the orthomosaic created from the drone imagery. Shrub areas (yellow polygons) were manually digitized on screen in ArcGIS and exported for extracting each shrub from the point cloud in R.

The dense point cloud generated from Metashape and AOI polygons were imported into RStudio (R Core Team, 2023) using the '*lidR'* package (Roussel et al., 2020, 2022a). The shapefile with polygons created in ArcGIS was imported using the '*sf'* package (Pebesma, 2018). The point cloud was clipped to polygons resulting in a unique point cloud for each field-measured shrub using package '*lidR'* (Roussel et al., 2020, 2022a). The result was a unique point cloud for each field-measured shrub. The clipped point cloud profiles of individual shrubs were imported into CloudCompare (version 2.12.4, http://www.cloudcompare.org/, accessed September 2022) for volume estimations. Two distinct methods were used to estimate shrub canopy volume: allometric and volumetric.

The allometric method replicates the field method by calculating canopy volume from user-measured height and canopy widths. To measure height and width, distances between points were measured for each shrub using the CloudCompare XY distance tool (Fig. 3a). First, the height of the shrub was estimated by measuring the distance from the lowest point to the highest point on the point cloud profile (Fig. 3b). We used two allometric methods to estimate canopy widths: 'CC-snap' and 'Top-down'. The 'CC-snap' method followed Karl et al. (2020), where the orientation functions in CloudCompare were used to 'snap' point cloud data sets to pre-defined views (i.e., viewing the shrubs from the side via a south-facing direction and east-facing direction). Distances between points for the 'CC-snap' method were measured at the widest part of the point cloud profile of the shrub assessed on-screen by the technician (Fig 3d). The 'top-down' method attempted to closely mimic the field-based measurements, where a top-down view was used as the fixed perspective in CloudCompare and the observer measured the longest canopy width (D_1, Fig. 3c) and width perpendicular to D_1 (D_2, Fig. 3c). Shrub canopy volumes for each allometric method were calculated using equation [2].

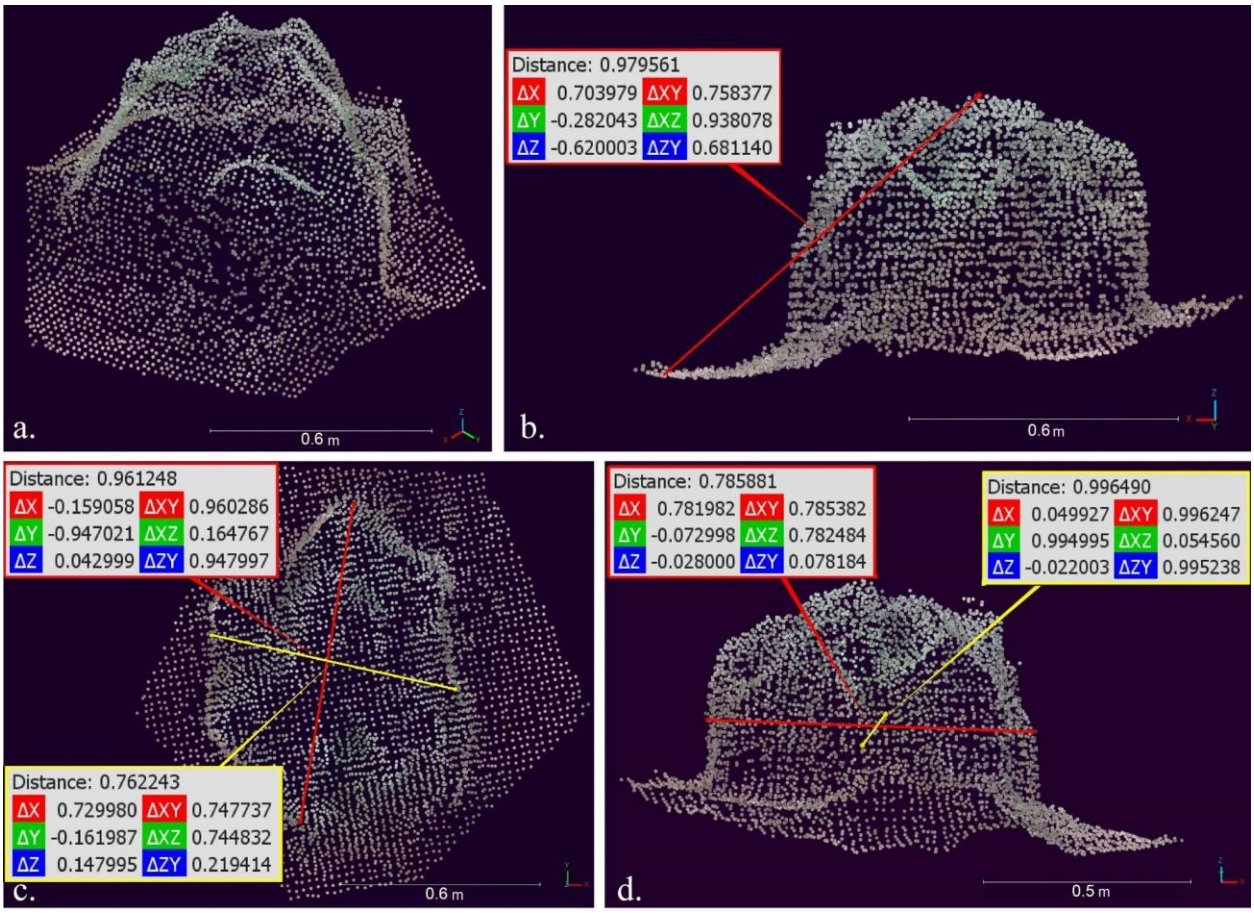

Figure 3. On-screen allometric methods to estimate volume of structure-from-motion-generated photogrammetric point cloud of each shrub (a) using the distance tool in CloudCompare. For both 'top-down' and 'CC-snap' methods, height (ΔZ) was measured by selecting a point from the top-most layer of the shrub canopy and a point from the lowest layer of the shrub canopy (connected by a red line; b). For the 'top-down' method (c), D_1 was the longest canopy width (red) and D_2 (yellow) was the greatest canopy width perpendicular to D_1. For the 'CC-snap' method (d), the shrub widths were measured using preset snap settings in CloudCompare with a south (red) and east view (yellow).

Volumetric methods used a generalized raster surface model of each shrub created by overlaying a grid on the point cloud and calculating shrub either mean or maximum height of each grid cell based on difference between the shrub model elevations and a fixed elevation (Karl et al., 2020). The fixed elevation value for each model was set to the minimum elevation (i.e., ground) of the point cloud data set of each shrub. Volume was estimated using two different cell dimensions (one side of each cell either 0.05m or 0.025m) and two height rules (average point height or maximum point height within each cell). Volumetric analysis was completed with CloudCompare using the 2.5D volume tool.

Statistical analysis was performed in R (version 4.0.3; R Core Team, 2021). Ordinary least-squares regression was used to compare field and drone-based estimates of shrub volume shrub height, and canopy widths. R^2 and slope values were used to compare different CloudCompare techniques to estimated volume and canopy width. We examined these trends across all species sampled, but also within each species to assess suitability of drone techniques for multiple upland sagebrush steppe shrub species across the range of size variability within

each species. Based on fundings by Karl et al. (2020), we expected that drone-based measurements of shrub canopy volume may be underestimated compared to field measurements, but still strongly correlated. Further, regression estimators could be used to estimate point cloud measurements with limited field data if there is a consistent relationship between field and drone estimates, and thus they will be reported here.

Allometric relationships to calculate aboveground biomass for eight rangeland shrubs using the SageSTEP network

Thirteen sites were sampled as part of the Sagebrush Steppe Treatment Project (SageSTEP; www.sagestep.org) network, established in 2006 (Fig. 4). SageSTEP is a collaborative research and management project designed to provide multisite, multidisciplinary, and long-term data on the outcomes of fuel reduction treatments covering a range of ecological conditions (McIver et al., 2014). The SageSTEP project consists of two networks of sites (shrubland and woodland) that were established to evaluate the response to woody vegetation removal over different environmental gradients. This research focuses on the "woodland" network, which examines the impacts of tree removal or redistribution over a piñon-juniper expansion gradient. Each of the 13 study sites sampled had between one to four dominant shrub species. Collectively, eight shrub species were sampled.

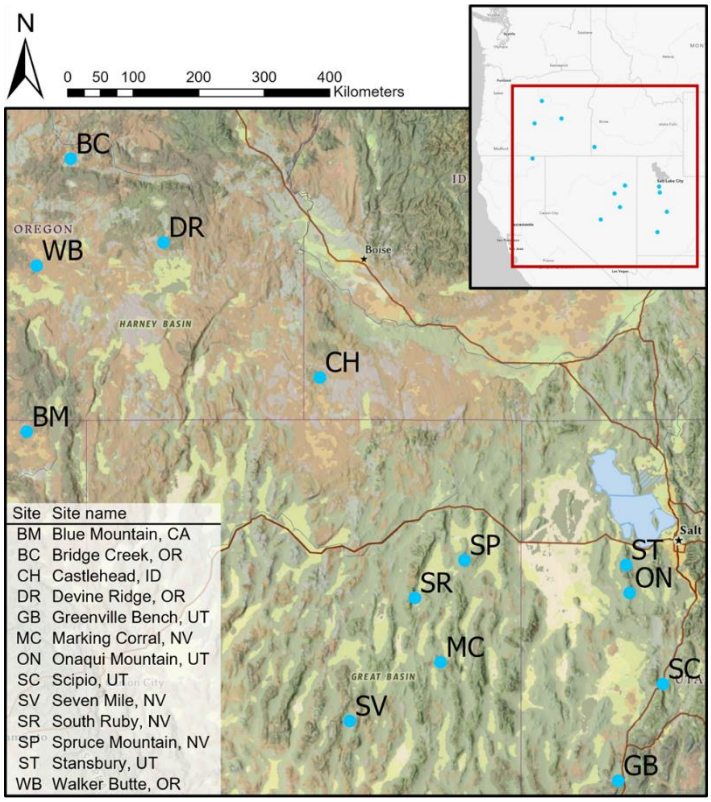

Figure 4. Sites within the SageSTEP Network that were included in this study.

At each site, representative individual shrubs of each dominant species, encompassing the range of sizes present at the site, were selected for destructive sampling. Only individuals outside of long-term study plots were sampled. Sample size ranged between 14 and 45 (median = 15) for each species at each site. Field sampling occurred April to August of 2006 and 2007.

Prior to shrubs being destructively harvested, the tallest height to the top of the foliage (not including inflorescence), longest canopy diameter, and perpendicular diameter were measured to the nearest whole centimeter. From height and canopy widths, canopy volume was calculated for each individual shrub using the equation for volume of an elliptical cone following Stebleton and Bunting (2009): $Volume = \frac{\pi}{6} * H * D_1 * D_2$, where H is shrub height to the top of the foliage, not including the inflorescence, D_1 is the longest canopy diameter, and D_2 is the longest diameter perpendicular to D_1.

Each shrub was then cut at the base and divided into 1- (0 to 0.6 cm), 10- (0.6 to 2.5 cm), and 100-hour (2.5 to 8 cm) fuel class components based on diameter (Lutes et al., 2006). Foliage was included as a part of the 1-hr fuel class. For each individual shrub, the plant material in each fuel class was weighed in the field to obtain a wet weight. Then, all plant material from the same species at the same site were pooled to create a wet fuel subset for each fuel class. These subsets were oven-dried at 50°C for 72 hours to obtain a dry mass. Percent mass for each fuel class was calculated as the subsample dry mass divided by the subsample wet mass. The percent mass for each species and site combination was multiplied by the individual shrub wet mass to obtain dry biomass for each individual shrub and each fuel class. Further, we also calculated percent composition for each fuel class as the relative mass of each fuels' class to total fuels per species.

From these field data, simple linear regressions were created to predict total dry biomass from field measured height, canopy diameters, and volume. Linear regression models were restricted such that the y-intercept was set to zero to match biological assumptions of no biomass when canopy biomass is zero. Regressions were built for each species and for each unique species and site combination, restricted to a minimum sample size of 5 for each site and species combination. We summarized model fit using an adjusted coefficient of determination (R^2), calculated using equation $R^2_{adj.} = 1 - (\frac{1-R^2}{n-p-1}) * (n-1)$, where R^2 is the R^2 value of the model, n is the number of observations, and p is the number of predictors (excluding the intercept).

To further assess model performance, we built models on only 90% of the available data (sampled with a random draw), leaving a reserve 10% for validation. From these reserve training points, we compared predicted (based on our linear regressions) versus observed dry biomass using two error metrics: Mean Absolute Error (MAE) and Root Mean Squared Error (RMSE). MAE was calculated as the average of the absolute differences between predicted and actual total dry biomass values in the validation set, providing an indication of the average magnitude of prediction errors. RMSE is the square root of the average of the squared differences between predicted and actual values, which gives greater weight to larger errors. Both metrics were used to evaluate the accuracy and reliability of the models in predicting biomass from field measurements.

Results and Discussion

A comparison and development of methods for estimating shrub volume using drone imagery-derived point clouds

All six point-cloud volume estimation techniques showed strong relationships between field- and point-cloud-estimated volume (Fig. 5). Among the two allometric methods, the CC-snap method outperformed the top-down method, by having both a better model fit (R^2 = 0.77 vs 0.74; Mean Square Error (MSE) = 0.0671 vs 0.0559) and slope closer to 1 (slope = 1 vs 0.88; Fig. 5).

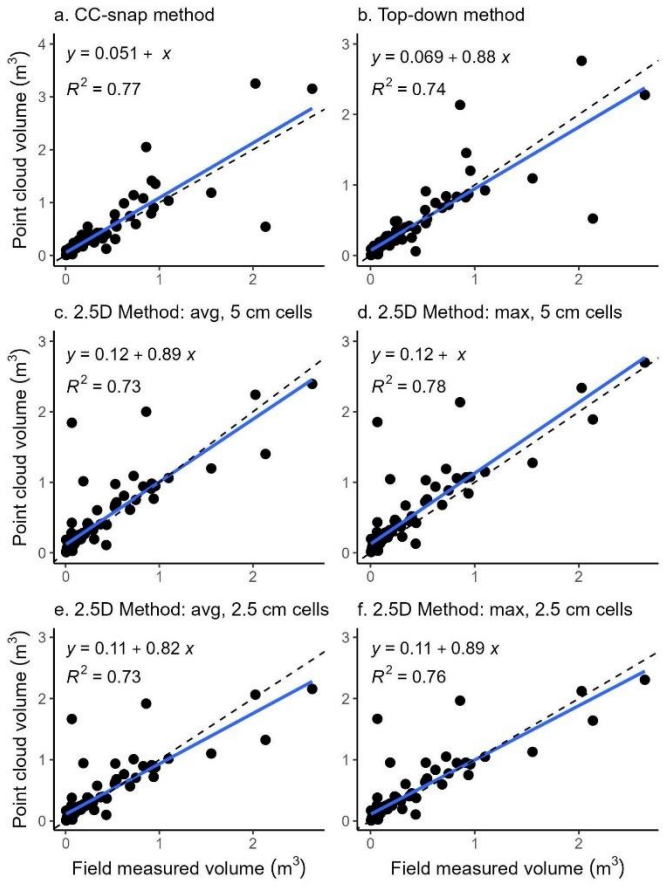

Figure 5. Comparing field and allometric (a-b) and volumetric (c-f) point cloud-based measurements of canopy volume. Model fit varied by shrub size: allometric methods better fit field estimates for smaller shrubs, whereas all 2.5D methods better fit field methods for larger (>1 m3) shrubs. All but two methods (a and d) underestimated canopy volume for larger shrubs and tended to slightly overestimate canopy volume for smaller shrubs. Blue line is linear regression line of best fit, dashed line is 1:1.

Canopy widths and height as measured with the two allometric methods can be directly compared to field measurements. CloudCompare estimates of height had good model fit to field measurements ($R^2 = 0.87$) but were slightly and consistently underestimated (slope = 0.91; Fig. 7). Model fit varied by shrub height. Shorter shrubs (field height <1m) had decreased model fit ($R^2 = 0.81$), but slope improved (slope = 0.96) compared to the model for all individuals, suggesting underestimation was greater for taller shrubs. CloudCompare allometric techniques better fit field measurements of D_1 (longest diameter) than D_2 (perpendicular to longest diameter). This difference suggests that field and CloudCompare techniques for identifying and measuring D_1 are more similar than those for D_2, potentially due to challenges to accurately identify perpendicularity to D_1 in the field. Within canopy width measurements, measurements of shrub canopy widths differed by CloudCompare allometric technique. The top-down method was better correlated to field measurements of D_1 than CC-snap ($R^2 = 0.75$ vs 0.72). Across both techniques, shrub widths <1 m were overestimated, and >1 m were underestimated. Model fit for allometric methods improved when only considering smaller shrubs (field volume < $1m^3$, 93% of individuals), suggesting that these methods are more consistent for smaller shrubs.

Among the volumetric techniques, all four iterations of the 2.5D method had similar and good model fit (R^2 range = 0.73 – 0.78; MSE range = 0.0501 – 0.06; Fig. 5). All but one (5 cm grid cells using maximum cell rule) of the 2.5D methods overestimated volume for shrubs <1 m^3, but underestimated volume for larger shrubs (Fig. 5). Volumetric methods with 2.5 cm cell dimensions had lower slopes than those from 5 cm grid dimensions, suggesting that a smaller cell size underestimated volume (Fig. 5). Within each cell dimensions, maximum cell rules yielded better model fit and slopes closer to 1 (Fig. 5). With volumetric techniques, maximum values from 5 cm grid cells performed best in terms of both R^2 (0.78), MSE (0.0591), and slope (1; Fig.5). Model fit for volumetric methods decreased when only considering smaller shrubs (field volume < $1m^3$, 93% of individuals), suggesting these methods provide more variable estimates for smaller shrubs.

Model fit by volume technique varied by species. In general, all point cloud estimates were best (in terms of R^2, MSE, and slope) for larger shrub species: *A. tridentata* subsp. *vaseyana*, *A. tridentata* subsp. *wyomingensis*, and *P. tridentata* (R^2 for volumetric techniques ≥ 0.92, MSE ≥ 0.02). Model fit for all six techniques was also good for *E. nauseosa* (R^2 = 0.82-0.86; MSE = 0.01 – 0.018). Model fit for *T. canescens* was good, but best for allometric methods (R^2 = 0.71-0.74 and 0.84-0.87 for volumetric and allometric methods, respectively; MSE < 0.001). Model fit was poorest for C. *viscidiflorus*, the smallest shrub species (maximum R^2 = 0.08, MSE = 0.15 – 0.34). Model fit for *A. arbuscula* was poor for all volumetric techniques (maximum R^2 = 0.19l; minimum MSE = 0.167) but moderate for allometric techniques (R^2 = 0.78 and 0.53; minimum MSE = 0.001).

Our results demonstrate measurements of upland sagebrush shrub species canopy volume from drone point clouds are a viable approach when compared with field-based estimates. We outlined non-destructive methods to consistently measure shrub canopy volume, which could be integrated into current rangeland monitoring programs (Gillan et al., 2020). This research improves upon techniques used by Cunliffe et al. (2021) and Karl et al. (2020) by sampling additional species and considering different techniques to measure point cloud canopy volume. Our results provide evidence for the suitability of measuring shrub canopy volume from drone point clouds for at least five upland sagebrush steppe shrubs: *A. tridentata* subsp. *tridentata*, *A. tridentata* subsp. *wyomingensis*, *E. nauseosa*, *P. tridentata*, and *T. canescens*. For these species, volume from drone point clouds was most like field-based measurements. Three of those five species, *A. tridentata* subsp. *vaseyana*, *A. tridentata* subsp. *wyomingensis*, and *P. tridentata*, are dominant at the study site and constitute significant proportions of woody fuel in sagebrush steppe ecosystems (Bourne and Bunting, 2011). Drone point cloud methods were not suitable to measure volume of two relatively small shrub species C. *viscidiflorus* and *A. arbuscula*. However, there was some variability in method suitability for in *A. arbuscula* as allometric methods were suitable, but volumetric methods were not.

One technique to potentially mitigate poor model fit for these smaller species is to consider alternate shapes for volume equations. To test if fit between field and point-cloud estimates could be improved especially for smaller species, we examined the results if volume (from field and allometric methods) was calculating using the equation for the volume of a cylinder $V = \pi * H * maximum(D_1, D_2)^2$, where radius is the greater measurement between D_1 and D_2. Using a cylinder resulted in minor improvements of R2 and MSE for C. *viscidiflorus* (ΔR^2 range from elliptical cone to cylinder = 0.068 – 0.175; ΔMSE range = -0.0004 – -0.0001). Similarly, model fit was marginally improved for volumetric methods of *A. arbuscula* (ΔR^2 range from elliptical cone to cylinder = 0.022 – 0.024; ΔMSE = -0.0058 – -0.0049). There were some improvements in model fit with this alternative shape, but model fit was poorer than that of suitable species using the original elliptical cone shape equation.

Suitability of allometric and volumetric methods differed by shrub size. Within allometric methods, drone-based techniques overestimated D_1 and D_2 for smaller shrubs (D_1 or D_2 <1 m). Smaller shrubs represented a majority of our sampling dataset (73% of shrubs had field measured D_1 <1m; 81% for D_2) due to our inclusion of multiple shrub species and attempts to sample across each species' size range. For shrubs with field-measured widths greater than 1m, point cloud estimates of width were more variable, and neither were consistently over nor

underestimated. Karl et al. (2020) implemented similar methods to estimate willow (*Salix* spp.) canopy volume from drone derived point clouds. However, they did not observe any bias based on size classes, which could be because the shrubs they studied were distributed more evenly across a wider size range, less variable, and generally larger in size (Karl et al. 2020). Finally, for the 'top-down' allometric technique, it is worth mentioning that this technique does not require the 3-D rendering of point cloud data on CloudCompare and could be executed using a 2-D (point-cloud derived) orthomosaic imagery on other image analysis or geospatial software. Allometric and volumetric methods can vary in their repeatability. Allometric methods require high amounts of user interaction and time, and we (similar to Karl et al. 2020) aimed to standardize these measurements using fixed views (CC-snap method). Volumetric methods, however, require relatively low amounts of manual interaction to obtain measurements and have the potential to be more easily standardized. Volumetric techniques were simpler and less time consuming to perform and would have less bias toward technician error or differences in judgement. Additionally, volumetric methods can be automated using a scripting-based approach (e.g., Greaves et al. (2015)).

We observed systematic model underestimation of shrub volume using point-cloud models. Karl et al. (2020) observed a similar trend and noted underestimation was likely due to dense vegetation obstructing bare ground and impeding the ability to model ground height. Understory vegetation height, especially when completely obstructing the ground surface, can be adjusted for in the model but may create additional variability in height estimates (see Karl et al. 2020). We suspect that the abundance of bare ground and deliberate vegetation removal around shrubs prior to drone data collection may have contributed to our improved accuracy in estimating height. We suspect that removing vegetation at the base of each shrub would not be necessary for future applications of these methods due to the natural abundance of bare ground as commonly seen in upland sagebrush communities (especially compared to riparian systems modeled by Karl et al. (2020)). Previous studies (Cunliffe et al., 2021) did not remove vegetation and still obtained highly accurate estimates of shrub biomass in semi-arid systems where some bare ground was present. Therefore, we do not believe that vegetation removal at the base of shrubs is necessary for all applications of these methods.

Further, it is important to consider how field methods may or may not translate to point cloud measurements and potentially lead to underestimation. In the field, canopy height and diameter are both measured along the greatest perennial, live plane of a shrub, which could be an individual branch depending on the shrub (Bonham, 2013; Bourne and Bunting, 2011). Points within the point cloud for that individual branch could be sparser or potentially even removed during the quality control and point filtering processes during model building. This means that estimates for that individual branch may not be included for both allometric and volumetric methods, and potentially contribute to underestimation compared to field estimates.
Our analysis focused on comparing point cloud and field measurements, but these are both estimates, and are indirect measures of volume. Field measurements are based on assumptions of canopy shape (in this case, an elliptical cone). This assumption confers inherent limitations, such as the top of each shrub is flat, the top is the maximum width, and there are no gaps within the canopy. Our allometric methods were also subject to these same assumptions. Volumetric methods were only partially limited as they allowed for differential heights but did not take into account gaps or decreases in canopy width throughout the plant. One potential benefit of point cloud data is the ability to adjust the classification and calculation methods to those which have

assumptions which are suitable for the analysis scenario. For example, another approach which could address some of these shape-based limitations is the voxel-counting method implemented by Greaves et al. (2015). Voxel-based approaches increment biomass into voxels, which are cubic volumes of space, or 3D pixels, and then calculate volume by counting the number of voxels for each shrub or across the region of interest. Voxel-counting methods may better account for canopy openings, but can be computationally more intensive than the methods we implemented (Greaves et al., 2015). Overall, it is important to consider assumptions and limitations of indirect measurements, especially those of field-based data, and drones may allow for greater flexibility in selecting an appropriate method with acceptable limitations.

An additional component of the study by Karl et al. (2020) was a cost-comparison of time spent on field measurements versus processing time of drone data for estimating canopy volumes. The study reported that collection of field measurements took more time (approximately 10 hours per sampling event for field-based measurements compared to about four hours per sampling event for drone-based estimates) than the photogrammetric estimations via drone data (Karl et al., 2020). While our study did not explicitly track time, similar outcomes can be inferred since the same model building methods were employed. Although the addition of GCPs added approximately one hour of time in the field (placing markers and recording RTK GNSS locations) and one hour of additional processing time (to identify marker locations in photos and rebuild models) in the lab, these points increased model accuracy and therefore were key to overlaying images/models over time in the same monitoring location.

Drones could also provide time savings if used in a double sampling technique. Double sampling requires that attributes be measured for all individuals using one technique, and a subset to be re-measured using a different technique (Karl et al., 2014). The sub-sampled method is generally more time and labor intensive but provides higher accuracy. A relationship between the sampling techniques methods is generated using linear regression analysis, and the fit or ability for the model to predict further outputs must be verified using reserved or new data (Karl et al., 2014). Although our study did not entail subsampling, such techniques could be implemented using drone estimates of shrub volume. Site and/or species-specific relationship could be derived to improve accuracy of drone-collected data, while maintaining the added benefit of increasing sample distribution with drones.

Drones offer comparable data products at a fractional cost of similar LiDAR outputs. Research by Olsoy (2014) explored the potential of terrestrial laser scanning (TLS), or ground-based LiDAR, in the same southern Idaho sagebrush ecosystem. In this study, sagebrush biomass was estimated from TLS-derived volume to detect seasonal variations in biomass. While TLS results are more accurate than those of airborne laser scanning (ALS) by way of generating denser point clouds, TLS instruments are bound to the same constraints as traditional field sampling in terms of site access and relative spatial coverage.

Allometric relationships to calculate aboveground biomass for eight rangeland shrubs using the SageSTEP network

A total of 631 individual shrubs of 8 species were sampled for this study. Average species shrub height ranged from 28 to 78 cm, and average species volume ranged from 36,147 to 1,156,611 cm^3 (Table 2).

Table 2. Summary of shrub size and biomass by species. Mean (minimum – maximum) values are displayed.

Species	n	Height (cm)	Diam1 (cm)	Diam2 (cm)	Volume (cm^3)	Dry biomass (g)
ARAR8	31	27.7 (11 - 47)	47.1 (18 - 80)	37.2 (5 - 80)	36147.2 (1084 - 159467)	204.1 (14 - 686)
ARNO4	64	35.0 (7 - 62)	53.4 (6 - 91)	44.1 (4 - 91)	61755.2 (88 - 321071)	395.5 (1 - 2151)
ARTRT	19	77.3 (15 - 210)	89.0 (8 - 266)	81.2 (5 - 266)	756947.8 (377 - 4536818)	1551.9 (2 - 7527)
ARTRV	100	66.4 (16 - 240)	79.8 (12 - 244)	62.4 (8 - 244)	420883.4 (804 - 7504511)	860.1 (7 - 7759)
ARTRW	145	57.0 (6 - 140)	69.1 (8 - 174)	58.0 (5 - 174)	227138.1 (151 - 1450885)	1081.3 (1 - 6662)
CHVI8	144	34.6 (10 - 130)	45.1 (10 - 95)	36.2 (5 - 95)	47727.1 (707 - 1007404)	128.1 (1 - 4884)
ERNA10	21	51.5 (17 - 86)	47.1 (13 - 87)	35.1 (12 - 87)	81306.9 (1620 - 331080)	481.7 (5 - 1382)
PUTR2	98	71.6 (12 - 217)	104.8 (10 - 244)	81.4 (10 - 244)	690805.2 (628 - 7504511)	1368.9 (4 - 8168)

Adjusted R^2 for species biomass equations, which related volume, height, and canopy diameters to dry biomass, ranged from 0.770 (*P. tridentata*) to 0.990 (*A. tridentata* ssp. *tridentata*; Table 3). Additionally, MAE ranged from 43.90 (*A. arbuscula)* to 1,653.61 g (*A. tridentata* ssp. *Tridentata*; Table 3). Biomass equations for each species are reported in Table 3. Adjusted R^2 for species by site biomass equations ranged from 0.490 to 1 and MAE ranged from 4.92 (*C. viscidiflorus* at Spruce Mountain, NV) to 1,821.95 g (*P. tridentata* at Stansbury, UT).

Table 3. Biomass (dry, g) model statements for each species by volume (cm^3), height (cm), diameter 1 (cm), and diameter 2 (cm).

Species	Model	R^2 adj. [1]	RMSE (g) [2]	MAE (g) [2]
ARAR8	biomass (g) = volume * 0 + height * -2.97 + diam1 * 4.2 + diam2 * -0.97	0.940	47.53	43.90
ARNO4	biomass (g) = volume * 0 + height * -7.92 + diam1 * 9.36 + diam2 * -2.28	0.920	90.33	73.28
ARTRT	biomass (g) = volume * 0 + height * -0.53 + diam1 * 3.77 + diam2 * 2.46	0.990	515.32	417.60
ARTRV	biomass (g) = volume * 0 + height * -4.78 + diam1 * 6.93 + diam2 * 3.67	0.840	3980.87	1653.61
ARTRW	biomass (g) = volume * 0 + height * 1.13 + diam1 * 7.29 + diam2 * -4	0.910	326.76	234.52
CHVI8	biomass (g) = volume * 0 + height * 0.83 + diam1 * 2.7 + diam2 * -6.87	0.950	79.22	48.71
ERNA10	biomass (g) = volume * 0 + height * 5.48 + diam1 * 11.49 + diam2 * -11.95	0.830	88.82	64.57
PUTR2	biomass (g) = volume * 0 + height * 20.15 + diam1 * -14.23 + diam2 * 16.64	0.770	646.76	563.00

[1] Adjusted R^2 value for full model statement, for significance and standard error values for each coefficient, see Table A.2.

[2] Both RMSE and MAE are calculated using a 10% leave out sample.

Though each species varied in total size, in general 1-hour fuels composed the least amount of total biomass, making up between 0.6 – 9.4% of total biomass depending on the species (Table 4; Fig. 6). Ten-hour fuels comprised between 11 – 42% of total biomass (Table 6; Fig. 2). Biomass was primarily composed of 100-hour fuels, accounting for between 43 – 88% of total biomass (Table 4; Fig. 6). Mass and composition by fuel class could be used to translate total biomass measurements into fuels classes using Table 4.

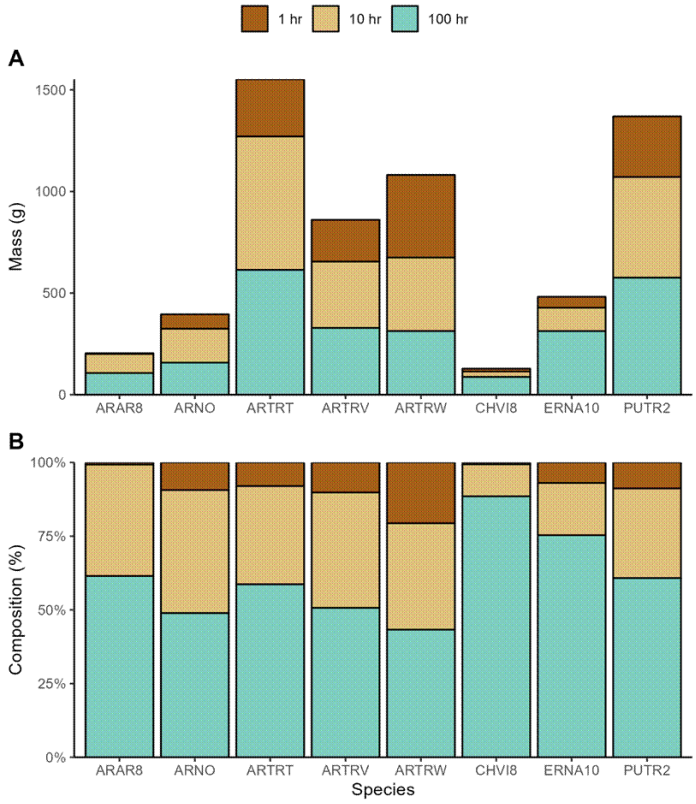

Figure 6. Fuel composition as mass (A) and percent composition (B) by fuel class for each shrub species.

We elected for consistency in our models across species and sites, and thus used linear regression equations which always included volume, height and canopy diameters as predictor variables. Other allometric methods (e.g., Grinath 2019) examined different combinations of predictor variables and model forms other than linear. The power in our modeling approach is based on robust field sampling. As a result, our models were completely based on field methods and thus error metrics we report are restricted to the range of sizes observed during field sampling (Table 2).

Table 4. Average dry mass and percent composition of total volume for each fuels class for each species.

Species	Fuels class	Dry mass (g) (± SE)	Composition (%) (± SE)
ARAR8	1 hr	3.76 (± 2.6)	0.73 (± 0.5)
	10 hr	93.62 (± 18.7)	37.77 (± 3.2)
	100 hr	106.7 (± 18.1)	61.5 (± 3.3)
ARNO4	1 hr	71.09 (± 16.9)	9.38 (± 1.6)
	10 hr	166.55 (± 23.8)	41.71 (± 1.7)

Species	Fuels class	Dry mass (g) (± SE)	Composition (%) (± SE)
	100 hr	157.86 (± 17.4)	48.91 (± 1.8)
ARTRT	1 hr	281.47 (± 158.2)	8 (± 2.6)
	10 hr	656.34 (± 245)	33.33 (± 3.6)
	100 hr	614.08 (± 177)	58.68 (± 4.5)
ARTRV	1 hr	205.37 (± 51.6)	10.18 (± 1.4)
	10 hr	326.32 (± 44.5)	39.13 (± 1.3)
	100 hr	328.45 (± 39.7)	50.69 (± 1.6)
ARTRW	1 hr	406.8 (± 57.8)	20.64 (± 1.8)
	10 hr	361.31 (± 37.1)	36.09 (± 1.2)
	100 hr	313.2 (± 29.1)	43.27 (± 1.7)
CHVI8	1 hr	13.87 (± 12.6)	0.64 (± 0.3)
	10 hr	26.7 (± 10.6)	10.85 (± 1.1)
	100 hr	87.56 (± 12.4)	88.51 (± 1.2)
ERNA10	1 hr	53.67 (± 17.5)	6.94 (± 2.3)
	10 hr	115.08 (± 26.7)	17.73 (± 3.8)
	100 hr	312.94 (± 72.1)	75.33 (± 4.6)
PUTR2	1 hr	297.97 (± 56.3)	8.81 (± 1.3)
	10 hr	495.22 (± 71.1)	30.42 (± 1.3)
	100 hr	575.72 (± 70.7)	60.77 (± 2)

Our findings both complement and can be compared to other allometric relationships in sagebrush-dominated ecosystems. For example, fit for models which translate crown volume of big sagebrush subspecies to aboveground biomass include 0.92 (adjusted R^2, as reported by Cleary et al. 2008) or 0.90 (R^2, as reported by Rittenhouse and Sneva 1977). These R^2 values are comparable to ours: we observed adj. R^2 = 0.840 and 0.910 for generalized species equations of *A. tridentata* ssp. *vaseyana* and *A. tridentata* ssp. *wyomingensis*, respectively. Similarly, we observed site-level model adj. R^2 ranging from 0.75-0.98 *A. tridentata* ssp. *vaseyana* and site-level = 0.90-0.98 for *A. tridentata* ssp. *wyomingensis*. Overall, we expand the species and site characteristics available for shrubland allometric equations. Those using allometric equations may select relationships which best meet their needs in terms of species and environmental site

coverage, model performance, and data access.

We provide relationships which relate biomass to field measured shrub size. However, unpersoned aerial vehicles (UAVs, i.e., drones) could also be used for non-destructive shrub sampling. Several studies have demonstrated the high value of drone-acquired imagery for sampling vegetation attributes (Cunliffe et al., 2021, 2016; Gillan et al., 2014; Karl et al., 2014). The availability of low-cost consumer UAVs with high-quality imaging sensors allows for very-high-resolution imagery to be easily and inexpensively collected. Further, new photogrammetric techniques can create high-quality 3-dimensional models and orthomosaics from drone imagery (Westoby et al., 2012). Altogether, these innovations have opened new possibilities for using UAVs as a supplement or replacement for field measurement methods, as demonstrated by Karl et al. (2020) in their measurements of willow canopy volume using drone-collected images and by Cunliffe et al. (2021) in estimating above-ground biomass of vegetation in arid ecosystems. UAV-based techniques measure volume within voxels (Greaves et al., 2015), or volume components (height, canopy widths; Harrison et al., 2024), all of which could be translated to total biomass and within fuels classes using the relationships we provide. UAV-based methods to estimate plant biomass are promising, but currently workflows to leverage UAV-based methods are inaccessible for land management application.

Conclusions (Key Findings) and Implications for Management/Policy and Future Research

This project is part of a growing collection of research in drone-based vegetation measurements that adds common sagebrush shrubland species to the species directory for drone methods (Cunliffe et al., 2021). Drone-imagery methods for rangeland monitoring have the potential to supplement or potentially replace field methods in some but not all instances (Gillan et al., 2020; Laliberte et al., 2011, 2010; Rango et al., 2009). Drone-based methods may also allow managers to estimate metrics not measurable from the ground and at sampling frequencies and extents not currently feasible, such as bare ground cover immediately post-wildfire or 3-D representations of canopy gaps (Gillan et al., 2020). Further refinements may be needed to develop methods for measuring low-stature species that showed lower accuracy in drone-measurements, notably *A. arbuscula* and C. *viscidiflorus*. Findings suggest that obtaining canopy volume using drones may be an attractive strategy for shrubland managers to expand their spatial catalogue and/or increase measurement frequency without increasing costs. Doing so would allow for more accurate monitoring of land cover changes that would highlight areas where management projects would be most impactful and further damage could be most effectively prevented.

Further, this project significantly contributes to the understanding of shrub biomass dynamics in sagebrush-dominated ecosystems, with a particular focus on the Great Basin region. We provide a versatile approach for estimating shrub biomass, using generalized species-specific and site-specific biomass relationships for eight shrub species. Additionally, we provide resources to translate total biomass into fuel size classes. The equations we provide could be used to generate total and fuels class biomass from measurements of shrub height and canopy diameter size or volume. Resulting biomass values can serve as valuable inputs into rangeland resource modeling, including fire behavior, wildlife habitat characteristics or forage production. Our allometric equations are built off the largest published dataset of its kind for rangeland shrubs, and we provide equations within an excel sheet and an R script to empower a broader

audience to apply these equations in real-world scenarios, fostering advancements in fire behavior assessment, ecological research, and land management practices in sagebrush shrubland ecosystems.

Literature Cited

Allred, B.W., Bestelmeyer, B.T., Boyd, C.S., Brown, C., Davies, K.W., Duniway, M.C., Ellsworth, L.M., Erickson, T.A., Fuhlendorf, S.D., Griffiths, T.V., Jansen, V., Jones, M.O., Karl, J., Knight, A., Maestas, J.D., Maynard, J.J., McCord, S.E., Naugle, D.E., Starns, H.D., Twidwell, D., Uden, D.R., 2021. Improving Landsat predictions of rangeland fractional cover with multitask learning and uncertainty. Methods Ecol Evol 12, 841–849. https://doi.org/10.1111/2041-210X.13564

Anderson, J.E., Inouye, R.S., 2001. Landscape-scale changes in plant species abundance and biodiversity of a Sagebrush Steppe over 45 years. Ecological Monographs 71, 531–556. https://doi.org/10.1890/0012-9615(2001)071[0531:LSCIPS]2.0.CO;2

Anderson, K., Gaston, K., 2013. Lightweight unmanned aerial vehicles will revolutionize spatial ecology. Frontiers in Ecology and the Environment 11, 138–146.

Anthony, C.R., Hagen, C.A., Dugger, K.M., Elmore, R.D., 2020. The effects of fire on the thermal environment of sagebrush communities. Journal of Thermal Biology 89, 102488. https://doi.org/10.1016/j.jtherbio.2019.102488

Bonham, C.D., 2013. Measurements for terrestrial vegetation, Second edition. ed. Wiley-Blackwell, Chichester, West Sussex, UK ; Hoboken, NJ.

Bourne, A., Bunting, S.C., 2011. Post-treatment Fuels in the Sagebrush Steppe and Juniper Woodlands of the Great Basin. (Technical Note No. 427). Bureau of Land Management, Denver, CO.

Cao, L., Liu, H., Fu, X., Zhang, Z., Shen, X., Ruan, H., 2019. Comparison of UAV LiDAR and Digital Aerial Photogrammetry Point Clouds for Estimating Forest Structural Attributes in Subtropical Planted Forests. Forests 10, 145. https://doi.org/10.3390/f10020145

Chambers, J.C., Brown, J.L., Bradford, J.B., Doherty, K.E., Crist, M.R., Schlaepfer, D.R., Urza, A.K., Short, K.C., 2023. Combining resilience and resistance with threat-based approaches for prioritizing management actions in sagebrush ecosystems. Conservat Sci and Prac 5, e13021. https://doi.org/10.1111/csp2.13021

Chambers, J.C., Brown, J.L., Reeves, M.C., Strand, E.K., Ellsworth, L.M., Tortorelli, C.M., Urza, A.K., Short, K.C., 2024a. Fuel treatment response groups for fire-prone sagebrush landscapes. Fire Ecology. 19: 70. 19, 70. https://doi.org/10.1186/s42408-023-00230-2

Chambers, J.C., Strand, E.K., Ellsworth, L.M., Tortorelli, C.M., Urza, A.K., Crist, M.R., Miller, R.F., Reeves, M.C., Short, K.C., Williams, C.L., 2024b. Review of fuel treatment effects on fuels, fire behavior and ecological resilience in sagebrush (Artemisia spp.) ecosystems in the Western U.S. Fire Ecology 20, 32. https://doi.org/10.1186/s42408-024-00260-4

Chambers, J.C., Urza, A.K., Board, D.I., Miller, R.F., Pyke, D.A., Roundy, B.A., Schupp, E.W., Tausch, R.J., 2021. Sagebrush recovery patterns after fuel treatments mediated by disturbance type and plant functional group interactions. Ecosphere 12, e03450. https://doi.org/10.1002/ecs2.3450

Chew, R.M., Chew, A.E., 1965. The Primary Productivity of a Desert-Shrub (Larrea tridentata) Community. Ecological Monographs 35, 355–375. https://doi.org/10.2307/1942146

Cleary, M.B., Pendall, E., Ewers, B.E., 2008. Testing sagebrush allometric relationships across three fire chronosequences in Wyoming, USA. Journal of Arid Environments 72, 285–

301. https://doi.org/10.1016/j.jaridenv.2007.07.013
CloudCompare (version 2.12.4), 2022. . GPL Software. Retrieved from http://www.cloudcompare.org/.
Cunliffe, A.M., Anderson, K., Boschetti, F., Brazier, R.E., Graham, H.A., Myers-Smith, I.H., Astor, T., Boer, M.M., Calvo, L.G., Clark, P.E., Cramer, M.D., Encinas-Lara, M.S., Escarzaga, S.M., Fernández-Guisuraga, J.M., Fisher, A.G., Gdulová, K., Gillespie, B.M., Griebel, A., Hanan, N.P., Hanggito, M.S., Haselberger, S., Havrilla, C.A., Heilman, P., Ji, W., Karl, J.W., Kirchhoff, M., Kraushaar, S., Lyons, M.B., Marzolff, I., Mauritz, M.E., McIntire, C.D., Metzen, D., Méndez-Barroso, L.A., Power, S.C., Prošek, J., Sanz-Ablanedo, E., Sauer, K.J., Schulze-Brüninghoff, D., Šímová, P., Sitch, S., Smit, J.L., Steele, C.M., Suárez-Seoane, S., Vargas, S.A., Villarreal, M., Visser, F., Wachendorf, M., Wirnsberger, H., Wojcikiewicz, R., 2021. Global application of an unoccupied aerial vehicle photogrammetry protocol for predicting aboveground biomass in non-forest ecosystems. Remote Sens Ecol Conserv 8, 57–71. https://doi.org/10.1002/rse2.228
Cunliffe, A.M., Brazier, R.E., Anderson, K., 2016. Ultra-fine grain landscape-scale quantification of dryland vegetation structure with drone-acquired structure-from-motion photogrammetry. Remote Sensing of Environment 183, 129–143. https://doi.org/10.1016/j.rse.2016.05.019
Davies, K.W., Boyd, C.S., Beck, J.L., Bates, J.D., Svejcar, T.J., Gregg, M.A., 2011. Saving the sagebrush sea: An ecosystem conservation plan for big sagebrush plant communities. Biological Conservation 144, 2573–2584. https://doi.org/10.1016/j.biocon.2011.07.016
Doherty, K., Theobald, D.M., Bradford, J.B., Wiechman, L.A., Bedrosian, G., Boyd, C.S., Cahill, M., Coates, P.S., Creutzburg, M.K., Crist, M.R., Finn, S.P., Kumar, A.V., Littlefield, C.E., Maestas, J.D., Prentice, K.L., Prochazka, B.G., Remington, T.E., Sparklin, W.D., Tull, J.C., Wurtzebach, Z., Zeller, K.A., 2022. A sagebrush conservation design to proactively restore America's sagebrush biome (No. 2022–1081), Open-File Report. U.S. Geological Survey. https://doi.org/10.3133/ofr20221081
Duarte, A., Borralho, N., Cabral, P., Caetano, M., 2022. Recent Advances in Forest Insect Pests and Diseases Monitoring Using UAV-Based Data: A Systematic Review. Forests 13, 911. https://doi.org/10.3390/f13060911
Ecke, S., Dempewolf, J., Frey, J., Schwaller, A., Endres, E., Klemmt, H.-J., Tiede, D., Seifert, T., 2022. UAV-Based Forest Health Monitoring: A Systematic Review. Remote Sensing 14, 3205. https://doi.org/10.3390/rs14133205
Ellsworth, L.M., Newingham, B.A., Shaff, S.E., Williams, C.L., Strand, E.K., Reeves, M., Pyke, D.A., Schupp, E.W., Chambers, J.C., 2022. Fuel reduction treatments reduce modeled fire intensity in the sagebrush steppe. Ecosphere 13. https://doi.org/10.1002/ecs2.4064
Germino, M.J., Torma, P., Fisk, M.R., Applestein, C.V., 2022. Monitoring for adaptive management of burned sagebrush-steppe rangelands: addressing variability and uncertainty on the 2015 Soda Megafire. Rangelands 44, 99–110. https://doi.org/10.1016/j.rala.2021.12.002
Gillan, J.K., Karl, J.W., Duniway, M., Elaksher, A., 2014. Modeling vegetation heights from high resolution stereo aerial photography: An application for broad-scale rangeland monitoring. Journal of Environmental Management 144, 226–235. https://doi.org/10.1016/j.jenvman.2014.05.028
Gillan, J.K., Karl, J.W., van Leeuwen, W.J.D., 2020. Integrating drone imagery with existing rangeland monitoring programs. Environ Monit Assess 192, 269.

https://doi.org/10.1007/s10661-020-8216-3
Greaves, H.E., Vierling, L.A., Eitel, J.U.H., Boelman, N.T., Magney, T.S., Prager, C.M., Griffin, K.L., 2015. Estimating aboveground biomass and leaf area of low-stature Arctic shrubs with terrestrial LiDAR. Remote Sensing of Environment 164, 26–35. https://doi.org/10.1016/j.rse.2015.02.023
Grinath, J.B., 2019. Comparing predictive measures and model functions for estimating plant biomass: lessons from a sagebrush–rabbitbrush community. Plant Ecology 220, 619–632.
Guimarães, N., Pádua, L., Marques, P., Silva, N., Peres, E., Sousa, J.J., 2020. Forestry Remote Sensing from Unmanned Aerial Vehicles: A Review Focusing on the Data, Processing and Potentialities. Remote Sensing 12, 1046. https://doi.org/10.3390/rs12061046
Harrison, G.R., Shrestha, A., Strand, E.K., Karl, J.W., 2024. A comparison and development of methods for estimating shrub volume using drone-imagery-derived point clouds. Ecosphere 15, e4877. https://doi.org/10.1002/ecs2.4877
Herrick, J.E., Van Zee, J.W., McCord, S.E., Ericha M., C., Karl, J.W., Burkett, L.M., 2017. Monitoring manual for grassland, shrubland, and savanna ecosystems, 2nd edition. ed. USDA - ARS Jornada Experimental Range, Las Cruces, N.M.
James, M.R., Robson, S., d'Oleire-Oltmanns, S., Niethammer, U., 2017. Optimising UAV topographic surveys processed with structure-from-motion: Ground control quality, quantity and bundle adjustment. Geomorphology 280, 51–66. https://doi.org/10.1016/j.geomorph.2016.11.021
Karl, J.W., Taylor, J., Bobo, M., 2014. A double-sampling approach to deriving training and validation data for remotely-sensed vegetation products. International Journal of Remote Sensing 35, 1936–1955. https://doi.org/10.1080/01431161.2014.880820
Karl, J.W., Yelich, J.V., Ellison, M.J., Lauritzen, D., 2020. Estimates of Willow (Salix Spp.) Canopy Volume using Unmanned Aerial Systems. Rangeland Ecology & Management 73, 531–537. https://doi.org/10.1016/j.rama.2020.03.001
Laliberte, A.S., Herrick, J.E., Rango, A., Winters, C., 2010. Acquisition, Orthorectification, and Object-based Classification of Unmanned Aerial Vehicle (UAV) Imagery for Rangeland Monitoring. photogramm eng remote sensing 76, 661–672. https://doi.org/10.14358/PERS.76.6.661
Laliberte, A.S., Winters, C., Rango, A., 2011. UAS remote sensing missions for rangeland applications. Geocarto International 26, 141–156. https://doi.org/10.1080/10106049.2010.534557
Li, W., Guo, Q., Jakubowski, M.K., Kelly, M., 2012. A New Method for Segmenting Individual Trees from the Lidar Point Cloud. photogramm eng remote sensing 78, 75–84. https://doi.org/10.14358/PERS.78.1.75
Li, Z., Shi, H., Vogelmann, J.E., Hawbaker, T.J., Peterson, B., 2020. Assessment of Fire Fuel Load Dynamics in Shrubland Ecosystems in the Western United States Using MODIS Products. Remote Sensing 12, 1911. https://doi.org/10.3390/rs12121911
Ludwig, J.A., Reynolds, J.F., Whitson, P.D., 1975. Size-biomass relationships of several Chihuahuan Desert shrubs. The American Midland Naturalist 92, 452–462.
Lutes, D.C., Keane, R.E., Caratti, J.F., Key, C.H., Benson, N.C., Sutherland, S., Gangi, L.J., 2006. FIREMON: Fire effects monitoring and inventory system (No. RMRS-GTR-164). U.S. Department of Agriculture, Forest Service, Rocky Mountain Research Station, Ft. Collins, CO. https://doi.org/10.2737/RMRS-GTR-164
McIver, J., Brunson, M., Bunting, S., Chambers, J., Doescher, P., Grace, J., Hulet, A., Johnson,

D., Knick, S., Miller, R., Pellant, M., Pierson, F., Pyke, D., Rau, B., Rollins, K., Roundy, B., Schupp, E., Tausch, R., Williams, J., 2014. A Synopsis of Short-Term Response to Alternative Restoration Treatments in Sagebrush-Steppe: The SageSTEP Project. Rangeland Ecology & Management 67, 584–598. https://doi.org/10.2111/REM-D-14-00084.1

Median, D.E., 1960. Pysical site factors influencing annual production of true mountain mahogany, Cercocarpus montanus. Ecology 41, 454–460.

Mohan, M., Leite, R.V., Broadbent, E.N., Jaafar, W.S.W.M., Srinivasan, S., Bajaj, S., Corte, A.P.D., Amaral, C.H. do, Gopan, G., Saad, S.N.M., Kamarulzaman, A.M.M., Prata, G.A., Llewelyn, E., Johnson, D.J., Doaemo, W., Bohlman, S., Zambrano, A.M.A., Cardil, A., 2021. Individual tree detection using UAV-lidar and UAV-SfM data: A tutorial for beginners. Open Geosciences 13, 1028–1039. https://doi.org/10.1515/geo-2020-0290

Olsoy, P., 2014. Aboveground total and green biomass of dryland shrub derived from terrestrial laser scanning. ISPRS Journal of Photogrammetry and Remote Sensing 88, 166–173. https://doi.org/10.1016/j.isprsjprs.2013.12.006

Padgett, P.E., 2020. Weeds, Wheels, Fire, and Juniper: Threats to Sagebrush Steppe (General Technical Report No. RMRSGTR-409). USDA Forest Service Rocky Mountain Research Station, Fort Collins, CO.

Pebesma, E., 2018. Simple Features for R: Standardized Support for Spatial Vector Data. The R Journal 10, 439–446.

Plowright, A., Roussel, J.-R., 2021. ForestTools: Analyzing Remotely Sensed Forest Data.

Prošek, J., Šímová, P., 2019. UAV for mapping shrubland vegetation: Does fusion of spectral and vertical information derived from a single sensor increase the classification accuracy? International Journal of Applied Earth Observation and Geoinformation 75, 151–162. https://doi.org/10.1016/j.jag.2018.10.009

Pyke, D.A., Shaff, S.E., Chambers, J.C., Schupp, E.W., Newingham, B.A., Gray, M.L., Ellsworth, L.M., 2022. Ten-year ecological responses to fuel treatments within semiarid Wyoming big sagebrush ecosystems. Ecosphere 13. https://doi.org/10.1002/ecs2.4176

R Core Team, 2023. R: A Language and Environment for Statistical Computing. R Foundation for Statistical Computing, Vienna, Austria.

Rango, A., Laliberte, A., Herrick, J.E., Winters, C., Steele, C., Browning, D., 2009. Unmanned aerial vehicle-based remote sensing for rangeland assessment, monitoring, and management. J. Appl. Remote Sens 3, 033542. https://doi.org/10.1117/1.3216822

Reis, S.A., Ellsworth, L.M., Kauffman, J.B., Wrobleski, D.W., 2019. Long-Term Effects of Fire on Vegetation Structure and Predicted Fire Behavior in Wyoming Big Sagebrush Ecosystems. Ecosystems 22, 257–265. https://doi.org/10.1007/s10021-018-0268-7

Riccardi, C.L., Prichard, S.J., Sandberg, D.V., Ottmar, R.D., 2007. Quantifying physical characteristics of wildland fuels using the Fuel Characteristic Classification System. Can. J. For. Res. 37, 2413–2420. https://doi.org/10.1139/X07-175

Rigge, M., Homer, C., Cleeves, L., Meyer, D.K., Bunde, B., Shi, H., Xian, G., Schell, S., Bobo, M., 2020. Quantifying Western U.S. Rangelands as Fractional Components with Multi-Resolution Remote Sensing and In Situ Data. Remote Sensing 12, 412. https://doi.org/10.3390/rs12030412

Rittenhouse, L.R., Sneva, F.A., 1977. A Technique for Estimating Big Sagebrush Production. Journal of Range Management 30, 68–70.

Roussel, J.-R., Auty, D., Coops, N.C., Tompalski, P., Goodbody, T.R.H., Meador, A.S.,

Bourdon, J.-F., de Boissieu, F., Achim, A., 2020. lidR: An R package for analysis of Airborne Laser Scanning (ALS) data. Remote Sensing of Environment 251, 112061. https://doi.org/10.1016/j.rse.2020.112061

Roussel, J.-R., documentation), D.A. (Reviews the, features), F.D.B. (Fixed bugs and improved catalog, segment_snags()), A.S.M. (Implemented wing2015() for, track_sensor()), B.J.-F. (Contributed to R. for, track_sensor()), G.D. (Implemented G. for, management), L.S. (Contributed to parallelization, code), S.A. (Author of the C. concaveman, 2022a. lidR: Airborne LiDAR Data Manipulation and Visualization for Forestry Applications.

Sandberg, D.V., Ottmar, R.D., Cushon, G.H., 2001. Characterizing fuels in the 21st Century. Int. J. Wildland Fire 10, 381. https://doi.org/10.1071/WF01036

Schuyler, E.M., Ellsworth, L.M., Sanchez, D.M., Whittaker, D.G., 2021. Forage Quality and Quantity in Migratory and Resident Mule Deer Summer Ranges. Rangeland Ecology & Management 79, 43–52. https://doi.org/10.1016/j.rama.2021.07.004

Shinneman, D.J., Aldridge, C.L., Coates, P.S., Germino, M.J., Pilliod, D.S., Vaillant, N.M., 2018. A conservation paradox in the Great Basin—Altering sagebrush landscapes with fuel breaks to reduce habitat loss from wildfire (No. 2018–1034), Open-File Report. U.S. Geological Survey. https://doi.org/10.3133/ofr20181034

Shinneman, D.J., Strand, E.K., Pellant, M., Abatzoglou, J.T., Brunson, M.W., Glenn, N.F., Heinrichs, J.A., Sadegh, M., Vaillant, N.M., 2023. Future Direction of Fuels Management in Sagebrush Rangelands. Rangeland Ecology & Management S1550742423000118. https://doi.org/10.1016/j.rama.2023.01.011

Shrestha A., Harrison, G. (2023). gharrison159/UAVShrubVolume: Release for Zendo v2 (v2.0). Zenodo. https://doi.org/10.5281/zenodo.10403045

Stebleton, A., Bunting, S., 2009. Guide for Quantifying Fuels in the Sagebrush Steppe and Juniper Woodlands of the Great Basin (Technical Note No. 430). Bureau of Land Management, Denver, CO.

Strand, E.K., Launchbaugh, K.L., Limb, R.F., Torell, L.A., 2014. Livestock Grazing Effects on Fuel Loads for Wildland Fire in Sagebrush Dominated Ecosystems. Journal of Rangeland Applications 1, 35–57.

Thorne, M.S., Skinner, Q.D., Smith, M.A., Rodgers, J.D., Laycock, W.A., Cerekci, S.A., 2002. Evaluation of a Technique for Measuring Canopy Volume of Shrubs. Journal of Range Management 55, 235. https://doi.org/10.2307/4003129

Uresk, D.W., Gilbert, R.O., Rickard, W.H., 1997. Sampling Big Sagebrush for Phytomass. Journal of Range Management 30, 311–314.

Ursic, K.A., Kenkel, N.C., Larson, D.W., 1997. Revegetation Dynamics of Cliff Faces in Abandoned Limestone Quarries. The Journal of Applied Ecology 34, 289. https://doi.org/10.2307/2404877

Van Dyke, F., Darragh, J.A., 2006. Short- and Long-term Changes in Elk Use and Forage Production in Sagebrush Communities Following Prescribed Burning. Biodivers Conserv 15, 4375–4398. https://doi.org/10.1007/s10531-005-4383-3

Weise, C.L., Brussee, B.E., Coates, P.S., Shinneman, D.J., Crist, M.R., Aldridge, C.L., Heinrichs, J.A., Ricca, M.A., 2023. A retrospective assessment of fuel break effectiveness for containing rangeland wildfires in the sagebrush biome. Journal of Environmental Management 341, 117903. https://doi.org/10.1016/j.jenvman.2023.117903

Westoby, M.J., Brasington, J., Glasser, N.F., Hambrey, M.J., Reynolds, J.M., 2012. ‘Structure-

from-Motion' photogrammetry: A low-cost, effective tool for geoscience applications. Geomorphology 179, 300–314. https://doi.org/10.1016/j.geomorph.2012.08.021
Williams, C.L., Ellsworth, L.M., Strand, E.K., Reeves, M.C., Shaff, S.E., Short, K.C., Chambers, J.C., Newingham, B.A., Tortorelli, C., 2023. Fuel treatments in shrublands experiencing pinyon and juniper expansion result in trade-offs between desired vegetation and increased fire behavior. fire ecol 19, 46. https://doi.org/10.1186/s42408-023-00201-7
Wright, C.S., 2013. Models for Predicting Fuel Consumption in Sagebrush-Dominated Ecosystems. Rangeland Ecology and Management 66, 254–266.
Young, D.J.N., Koontz, M.J., Weeks, J., 2022. Optimizing aerial imagery collection and processing parameters for drone-based individual tree mapping in structurally complex conifer forests. Methods Ecol Evol 13, 1447–1463. https://doi.org/10.1111/2041-210X.13860
Zhao, Y., Liu, X., Wang, Y., Zheng, Z., Zheng, S., Zhao, D., Bai, Y., 2021. UAV-based individual shrub aboveground biomass estimation calibrated against terrestrial LiDAR in a shrub-encroached grassland. International Journal of Applied Earth Observation and Geoinformation 101, 102358. https://doi.org/10.1016/j.jag.2021.102358